

# Structural study, NCA, FT-IR, FT-Raman Spectral Investigations, NBO Analysis and Thermodynamic Functions of 1-Hydroxynaphthalene-2-Carboxylicacid

B. Raja<sup>1</sup>, V. Balachandran<sup>2\*</sup>, B. Narayana<sup>3</sup> and B.Revathi<sup>2</sup>

<sup>1</sup>Department of Physics, Government Arts College, Kulithalai-639120, Karur, India.

<sup>2</sup>Research Department of Physics, A. A. Government Arts College, Musiri-621211, India.

<sup>3</sup>Department of Studies in Chemistry, Mangalore University, Mangalagangothri-574 199, India.

## ARTICLE INFO

### Article history:

Received: 12 September 2016;

Received in revised form:

17 October 2016;

Accepted: 24 October 2016;

### Keywords

1-Hydroxynaphthalene-2-Arboxylicacid,  
Vibrational Spectra,  
NBO,  
HOMO-LUMO,  
MEP Surface.

## ABSTRACT

In this work, the vibrational characteristics of 1-hydroxynaphthalene-2-carboxylicacid (1HN2CA) have been investigated and both the experimental and theoretical vibrational data indicate the presence of functional groups in the title molecule. The density functional theoretical (DFT) computations were performed at the B3LYP/(ccPVDZ, 6-311+G(d)) levels to derive the optimized geometry, vibrational wavenumbers with IR and Raman intensities. Furthermore, the molecular orbital calculations such as natural bond orbital's (NBOs), HOMO-LUMO energy gap and Mapped molecular electrostatic potential (MEP) surfaces were also performed with the same level of DFT. The thermal flexibility of molecule in associated with vibrational temperature was also illustrated on the basis of correlation graphs. The detailed interpretation of the vibrational spectra has been carried out with the aid of potential energy distribution (PED) results obtained quantum chemical calculations. The delocalization of electron density of various constituents of the molecule has been discussed with the aid of NBO analysis.

© 2016 Elixir All rights reserved.

## Introduction

Naphthalene and its derivatives are biologically, pharmaceutically and industrially useful compounds. The structure of naphthalene is benzene-like, having two-six membered rings fused together. Particularly, naphthalene was studied because, of its technological applications in a vast amount of industrial process. In fact, it was used as a precursor for the synthesis of plastics and dyes, gamma-ray detector in photomultiplier tubes and also used in dye stuffs, synthetic resins, coatings, tanning agent and celluloid. Modern vibrational spectrometry has proven to be an exceptionally powerful technique for solving many chemical problems. It has been extensively employed both in the study of chemical kinetics and chemical analysis.

However, for a proper understanding of IR and Raman, a reliable assignment of all vibrational band is essential. Recently, computational methods based on density functional theory (DFT) are becoming widely used [1-4]. These methods predict relatively accurate molecular structure and vibrational spectra with moderate computational effort. In particular, for polyatomic molecules (typically normal modes exceeding 50) the DFT methods lead to the prediction of more accurate molecular structure and vibrational frequencies than the conventional ab initio restricted Hartree-Fock (RHF) and Moller-plestet second order perturbation theory (MP2) calculations. Among the DFT calculation, Becke's three parameter hybrid functional combined with the Lee-Yang-Parr correlation functional (B3LYP) is the best in predicting results for molecular geometry and vibrational wave numbers for moderately larger molecules [5-10].

To gain a better understanding of the performance and limits of DFT methods as a general approach to the vibrational problems of organic molecules, we calculated harmonic frequencies of 1-hydroxynaphthalene-2-carboxylicacid (1HN2CA) by DFT method, and compared these results with observed fundamental vibrational frequencies. The aim of this work is to check the performance of B3LYP density functional force field for simulation of IR and Raman spectra of the title compound with the use of standard ccPVDZ and 6-311+G(d) basis sets.

## Experimental Details

1HN2CA was provided by Lancaster Chemical Company, UK. which is of spectroscopic grade and hence used for recording the spectra as such without any further purifications. The room temperature Fourier Transform infrared spectrum of 1HN2CA was measured in the 4000-450 cm<sup>-1</sup> region at a resolution of ± 1cm<sup>-1</sup> using BRUKER IFS-66V FT-IR Spectrometer equipped with a KBR pellets were used in the spectral measurements. The FT-Raman spectrum was recorded on a BRUKER IFS-66V model interferometer equipped with an FRA-106 FT-Raman accessories in the 4000-100 cm<sup>-1</sup> stokes region using the 1064nm line of an Nd: YAG laser for excitation operating at 200mW Power.

## Computational Details

Analysis of molecular geometry optimizations, energy, and vibrational frequencies was carried out with the Gaussian 09 software package [11] at the DFT (B3LYP) levels supplemented with the standard ccPVDZ and 6-311+G(d) basis sets. Cartesian representation of the theoretical force constants has been computed at optimized geometry. Vibrational Modes

Tele:

E-mail address: [brsbala@rediffmail.com](mailto:brsbala@rediffmail.com)

were assigned by means of visual inspection using the GAUSSVIEW [12] program. Data revealed that DFT calculations using a basis set incorporating polarized functions yielded results that are in better agreement with the experimental data. For the plots of simulated IR and Raman spectra, pure Lorentzian band shapes were used with a band width of  $\pm 1 \text{ cm}^{-1}$ . Prediction of Raman intensities was carried out by the following procedure. The Raman activities ( $S_i$ ) calculated by the Gaussian 09 program were converted to relative Raman intensities ( $I_i$ ) using the following relationship derived from the basic theory of scattering.

$$I_i = \frac{f(\nu_0 - \nu_i)^4 S_i}{\nu_i [1 - \exp(-\frac{hc\nu_i}{kt})]} \dots\dots\dots (1)$$

Where  $\nu_0$  is the exciting wave number ( $\text{cm}^{-1}$  units)  $\nu_i$  is the vibrational wave number of the  $i^{\text{th}}$  normal mode,  $h$ ,  $c$  and  $k$  are universal constant and  $f$  is a suitably chosen common normalization factor for all peak intensities.

Natural bond orbital analysis (NBO) was also performed by the Gaussian 09 W program at the B3LYP level of theory analysis transforms the canonical delocalized Hartree-Fock (HF) Molecular orbital's (MO) into localized MOs that are closely tied to chemical bonding concepts. This process involves sequential transformation of non-orthogonal Atomic orbital's (AOs) to the sets of Natural atomic orbital's (NAOs), Natural hybrid orbital's (NHOs) Natural bond orbital's (NBOs). The localized basis sets are completely described the wave functions in the most economic method, as electron density and other properties that are described by the minimum amount of filled NBO. The interaction between filled and anti-bonding (or) Rydberg orbital's represented the deviation of the molecule from the Lewis structure and be used as the measure of delocalization. This non-covalent bonding anti-bonding charge transfer interactions can be quantitatively described in terms of the second order perturbation interaction energy ( $E^{(2)}$ ) [13-16]

#### Molecular geometry

The molecular structure of a 1HN2CA along with numbering of atoms is shown in Fig. 1. The maximum number of potentially active observable fundamentals of a non-linear molecule that contains  $N$  atoms is equal to  $(3N-6)$ , apart from three translational and three rotational degrees of freedom [17]. 1HN2CA having 22 atoms with 60 Normal modes of vibrations which are distributed amongst the symmetry species as  $(3N-6)_{\text{vib}}=41A'$  (in-plane) + 19  $A''$ (out-of-plane). The  $A'$  vibrations are totally symmetric and give rise to polarized Raman lines whereas  $A''$  vibrations are anti-symmetric and give rise to depolarized Raman lines. Figs.2 and 3 shows the observed and calculated B3LYP/ccPVDZ and B3LYP/6-311+G(d)FT-IR and FT-Raman spectra of 1HN2CA, respectively

#### Results and Discussion

The most optimized geometrical parameters (bond length, bond angle and dihedral angle) were calculated by B3LYP/ccPVDZ and B3LYP/6-311+G(d)basis sets which are depicted in Table 1.

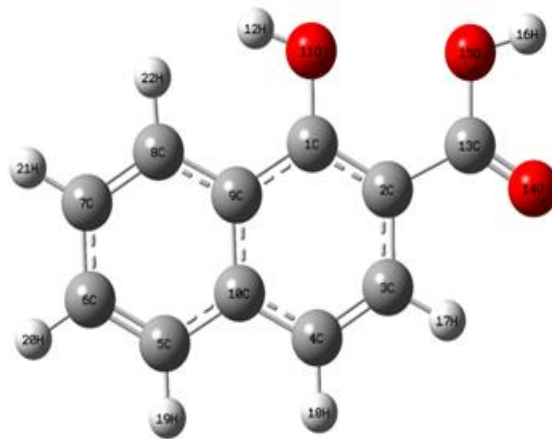


Fig 1. Optimized geometrical structure and atomic labeling of 1-hydroxy naphthalene 2-carboxylic acid

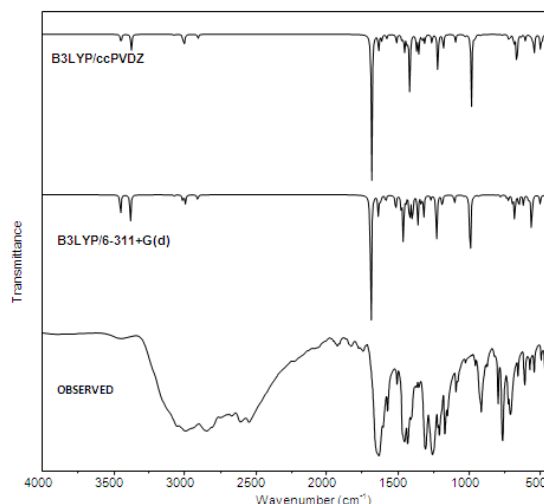


Fig 2. Observed and simulated FT-IR spectra of 1-hydroxynaphthalene 2-carboxylic acid

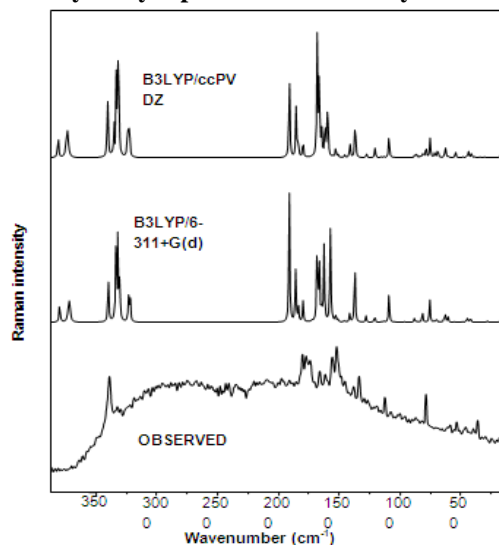


Fig 3. Observed and simulated FT- Raman spectra of 1-hydroxynaphthalene 2-carboxylic acid.

#### Vibrational Assignments

The detailed vibrational analysis of fundamental modes of 1HN2CA along with the FT-IR and FT-Raman experimental frequencies and the unscaled and scaled vibrational frequencies using B3LYP/ccPVDZ and B3LYP/6-311+G(d)basis sets are presented in Table 2.

### C–H Vibrations

Aromatic compounds commonly exhibit multiple weak bands in the region 3100–3000  $\text{cm}^{-1}$  due to aromatic C–H stretching vibrations [18–21] the bands appeared at 2992  $\text{cm}^{-1}$  in FT-IR spectrum and 3066, 3006, 2982, 2912  $\text{cm}^{-1}$  in FT-Raman spectrum are assigned to C–H ring stretching vibrations. The band identified at 3068, 3008, 2990, 2982, 2915, 2902  $\text{cm}^{-1}$  in B3LYP/6-31ccPVDZ and 3068, 3005, 2995, 2980, 2913, 2900  $\text{cm}^{-1}$  in B3LYP/6-311+G(d) methods are assigned to C–H ring stretching vibrations. The C–H in-plane and out-of-plane bending vibrations generally lie in the range 1000–1300  $\text{cm}^{-1}$  and 950–800  $\text{cm}^{-1}$  [22, 23], respectively. In the present case, six C–H in-plane bending vibrations of the title compound identified at 1028, 882, 874, 802, 686, 670  $\text{cm}^{-1}$  in B3LYP/6-31ccPDZ and 1025, 877, 868, 795, 681, 663  $\text{cm}^{-1}$  in B3LYP/6-311+G(d) methods are assigned to C–H in-plane bending vibrations. The C–H out-of-plane bending vibrations are observed at 492, 464  $\text{cm}^{-1}$  in FT-IR spectrum and 350, 263, 225, 71  $\text{cm}^{-1}$  in FT-Raman spectrum. According to the literature, the in-plane and out-of-plane bending vibrations are found to be lower than their characteristic regions due to the substitution of the OH.

### CC Vibrations

There are six equivalent C–C bonds in benzene and consequently there will be six C–C stretching vibrations. In addition there are several in-plane and out-of-plane bending vibrations of the ring C–C carbons. However due to this symmetry of benzene many modes of vibrations are IR active. In general the fundamental vibrational modes of C–C stretching generally occurred in the region 1600–1400  $\text{cm}^{-1}$  [20]. In the present work the wave numbers observed in the FT-IR spectrum of 1HN2CA at 1633, 1572, 1505, 1452, 1386, 1352, 1305, 1256, 1217  $\text{cm}^{-1}$  and FT-Raman spectrum of 1HN2CA at 1634, 1607, 1577, 1506, 1466, 1382, 1320, 1257, 1216  $\text{cm}^{-1}$  have been assigned to C–C stretching vibrations. The C–C stretching vibrations appears in the FT-IR spectrum at 1506  $\text{cm}^{-1}$  the theoretically computed values by the B3LYP/ccPVDZ method which are 1630, 1614, 1578, 1508, 1436, 1390, 1260, 1220  $\text{cm}^{-1}$  show an excellent agreement with experimental data. These modes of C–C stretching vibrations are found to have a PED contribution of 92% - 85% along with the in-plane bending modes.

The out-of-plane bending vibration is assigned to the band of 163  $\text{cm}^{-1}$ . In general C–C in-plane and out-of-plane bending vibrations calculated by B3LYP/ccPVDZ and B3LYP/ccPVTZ methods show good agreement with recorded spectra.

### Ring Vibrations

In the present work the wave numbers are observed in the FT-IR spectrum of title molecule at 912, 762, 722, 708, 604  $\text{cm}^{-1}$  and FT-Raman spectrum at 916, 722, 600  $\text{cm}^{-1}$  have been assigned to Ring in-plane bending and out-of-plane bending vibrations. The computed values are 922, 769, 726, 714, 648, and 608  $\text{cm}^{-1}$  are assigned to Ring in-plane bending vibrations. The bands identified at 568, 547, 490, 415, 316, and 292  $\text{cm}^{-1}$  are assigned to Ring out-of-plane bending vibrations. The in-plane bending vibrations are slightly below the expected range. This is due to the replacement of C by hydroxyl these assignments are line with the literature [24–26].

### OH Vibrations

The OH group vibrations are likely to be most sensitive to the environment, so they show pronounced shifts in the spectra of the hydrogen-bonded species. In the case of unsubstituted phenol it has been shown that the frequency of

OH stretching vibration in the gas phase is 3657  $\text{cm}^{-1}$  [27]. In our case a band in FT-IR spectrum 3443  $\text{cm}^{-1}$  is assigned to OH stretching vibration. A comparison of these bands with literature data predict that there is negative deviation of  $\sim 652 \text{ cm}^{-1}$  may be due to fact that the presence of strong intra-molecular hydrogen bonding. However, the calculated value by B3LYP/6-311+G(d) level shows at 3440  $\text{cm}^{-1}$ . The OH in-plane bending vibration in phenol, in general, lies in the region 1150–1250  $\text{cm}^{-1}$  and is not much affected due to hydrogen bonding unlike the stretching and out-of-plane deformation frequencies. The medium intense FT-IR frequency at 1090  $\text{cm}^{-1}$  is attributed to in-plane bending vibration. The theoretically computed value at 1094, 1092  $\text{cm}^{-1}$  by B3LYP, method coincides with experimental observation.

The OH out-of-plane deformation vibration in phenol lies in the region 290–320  $\text{cm}^{-1}$  for free OH and in the region 517–710  $\text{cm}^{-1}$  for associated OH [28]. In both inter-molecular and intra-molecular associations, the frequency is at a higher value than in free OH. The frequency increases with hydrogen bond strength because of the larger amount of energy required to twist the O–H bond out-of plane [29]. In the present case, the weak FT-IR band at 571  $\text{cm}^{-1}$  are observed, and these are attributed to OH out-plane bending vibration.

### COOH Vibrations

Carboxylic acid dimer is formed by strong hydrogen bonding in the solid state. Vibrational analysis of carboxylic acid group is made on the basis of carbonyl group and hydroxyl group. The C=O stretch of carboxylic acid is identical to the C=O stretch in ketones, which is expected in the region 1740–1660  $\text{cm}^{-1}$  [30]. The C=O bond formed by  $\text{P}\pi\text{--P}\pi$  between C and O, intermolecular hydrogen bonding reduces the frequencies of the C=O stretching absorption to a greater degree than does intermolecular H bonding because of the different electro negatives of C and O, the bonding is not equally distributed between the two atoms. The lone pair of electrons on oxygen also determines the nature of the carbonyl group. In our present study, very strong intense band observed in FT-Raman spectrum at 1681, 1414  $\text{cm}^{-1}$  and FTIR spectrum at 1430, 1412  $\text{cm}^{-1}$  is assigned to C=O stretching vibration while the ccPVDZ, scaled value at 1682, 1436, 1410  $\text{cm}^{-1}$  6-311+G(d) scaled value at 1680, 1432, 1413  $\text{cm}^{-1}$  and respectively are assigned to C=O stretching vibration for our title molecule. The computed an harmonic frequency nearly coincides with the experimental spectrum.

The free hydroxyl group absorbs strongly in the region 3700–3584  $\text{cm}^{-1}$ , where as the existence of intermolecular hydrogen bond formation can lower the O–H stretching frequency in the range 3500–3200  $\text{cm}^{-1}$  with increase in intensity and breadth [31,32]. The calculated wave number at 3376, 3368  $\text{cm}^{-1}$  in ccPVDZ and 6-311+G(d) methods, respectively, shows deviation when we compared with recorded FT-IR spectra and a weak FT-Raman spectral value at may be due to the presence of strong intermolecular hydrogen bonding to the neighboring carbonyl group. The in plane O–H deformation vibration usually appears as strong band in the region 1445–1260  $\text{cm}^{-1}$  in the FT-Raman spectrum [33]. The theoretically predicted band at 1180  $\text{cm}^{-1}$  in ccPVDZ, and 1178  $\text{cm}^{-1}$  in 6-311+G(d) is assigned to in-plane bending vibration of O–H group for title molecule is in good agreement with recorded FT-Raman band at 1178  $\text{cm}^{-1}$ . The O–H out-of-plane deformation vibration lies in the region 280–312  $\text{cm}^{-1}$  for free O–H and in the region 600–720  $\text{cm}^{-1}$  for associated O–H [22].

**Table 1. Optimized geometrical parameters of 1-hydroxy naphthalene 2-carboxylic acid by B3LYP/ccPVdZ and B3LYP/6-311+G(d).**

Parameters	Bond length		Parameters	Bond angle	
	B3LYP/ ccPVDZ	B3LYP/6-311+G(d)		B3LYP/ ccPVDZ	B3LYP/6-311+G(d)
C1-C2	1.40	1.39	C2-C1-C9	120.12	120.34
C1-C9	1.44	1.44	C2-C1-O11	119.67	119.42
C1-O11	1.35	1.35	C9-C1-O11	120.21	120.24
C2-C3	1.43	1.42	C1-C2-C3	119.10	118.94
C2-C13	1.49	1.49	C1-C2-C13	125.69	125.92
C3-C4	1.37	1.37	C3-C2-C13	115.20	115.14
C3-H17	1.09	1.08	C2-C3-C4	122.10	122.12
C4-C10	1.42	1.42	C2-C3-H17	116.47	116.90
C4-H18	1.09	1.08	C4-C3-H17	121.43	120.98
C5-C6	1.38	1.37	C3-C4-C10	120.11	120.20
C5-C10	1.42	1.42	C3-C4-H18	120.72	120.54
C5-H19	1.09	1.09	C6-C5-C10	119.17	119.26
C6-C7	1.42	1.41	C6-C5-H19	121.29	121.27
C6-H20	1.09	1.09	C10-C5-H19	120.35	120.27
C7-C8	1.38	1.38	C5-C6-C7	118.36	118.46
C7-H21	1.09	1.08	C5-C6-H20	120.03	119.98
C8-C9	1.42	1.42	C7-C6-H20	120.21	120.24
C8-H22	1.09	1.09	C6-C7-C8	119.76	119.78
C9-C10	1.43	1.43	C6-C7-H21	120.03	120.13
O11-H12	0.99	0.96	C8-C7-H21	120.01	119.97
C13-O14	1.22	1.21	C7-C8-H19	119.96	119.90
C13-O15	1.35	1.35	C7-C8-H22	121.39	121.39
O15-H16	0.98	0.97	C7-C8-H22	117.57	117.22
			C9-C8-H22	121.04	121.39
			C1-C9-C8	122.34	122.64
			C1-C9-C10	119.22	119.05
			C8-C9-C10	118.44	118.31
			C4-C10-C5	121.85	121.73
			C4-C10-C9	119.34	119.35
			C5-C10-C9	118.81	118.92
			C1-O11-H12	109.00	110.67
			C2-C13-O14	123.21	123.19
			C2-C13-O15	115.44	115.64
			O14-C13-O15	121.35	121.16
			C13-O15-H16	104.45	106.07

The recorded spectrum at  $541\text{ cm}^{-1}$  in FT-IR spectrum is assigned to O-H out-of-plane bending vibration with PED contribution of 67%. In the present molecule, the C-COOH stretching vibration is found with very strong intensity at  $1217\text{ cm}^{-1}$  in IR and medium band at  $1216\text{ cm}^{-1}$  in Raman which clearly indicates that its dipole bond character. The C-COOH in-plane vibration assigned at  $708\text{ cm}^{-1}$  and out-of-plane vibration assigned at  $160\text{ cm}^{-1}$  in B3LYP/ccPVDZ method,. The above results are in good agreement with the literature [34].

#### Natural Bond Orbital Analysis

Natural bond orbital (NBO) method encompasses a suite of algorithms that enable fundamental bonding concepts to be extracted from density functional theory (DFT) computation. Natural bond orbital analysis originated as a technique for studying hybridization and covalence effects in polyatomic wave functions based on local block Eigen vectors of the one-particle density matrix. NBOs would correspond closely to the picture of localized bonds and lone pairs as basic units of molecular structure. The atomic charges of 1HN2CA calculated by NBO analysis using the B3LYP/ccPVDZ method are presented in Table 3. Among the ring carbon atoms C1 of 1HN2CA have positive charges in B3LYP

method. The positive charge on C1 is due to the attachment of highly electronegative hydroxyl to it. In 1HN2CA compound carbon attached with the carboxyl group has negative NBO charge. This is due to the electron withdrawing nature of the carboxyl group by means of resonance.

#### Donor-Acceptor Interactions: Perturbation Theory Energy Analysis

NBO analyses of molecule illustrate the deciphering of the molecular wave function in terms Lewis structures, charge, bond order, bond type, hybridization, resonance, donor-acceptor interactions, etc.

The localized orbitals in the Lewis structure of 1HN2CA can interact strongly. These interactions can strengthen and weaken bonds. A lone pair donor  $\rightarrow$  antibonding acceptor orbital interaction will weaken the bond associated with the anti-bonding orbital. Conversely, an interaction with a bonding pair will strengthen the bond. Strong electron delocalization in the Lewis structure also shows up as donor-acceptor interactions. This calculation is done by examining all possible interactions between 'filled' (donor) Lewis-type NBOs and 'empty' (acceptor) non-Lewis NBOs, and estimating their energetic importance by second order perturbation theory.

**Table 2. Vibrational assignments of fundamental observed frequencies and calculated frequencies of 1-hydroxy naphthalene 2-carboxylic acid by B3LYP/ccPVDZ and B3LYP/6-311+G(d).**

Mode No.	Symmetry species	Observed frequencies		Calculated frequencies				Infrared intensities		Raman intensities		Vibrational assignments / (%)
		FT-IR	FT-Raman	Unscaled		Scaled		B3LYP / ccPVD Z	B3LYP/ 6-311+G(d)	B3LYP / ccPVD Z	B3LYP/ 6-311+G(d)	
				B3LYP/ ccPVDZ	B3LYP/ 6-311+G(d)	B3LYP / ccPVD Z	B3LYP/ 6-311+G(d)					
1	A'	3443		3789	3803	3446	3440	55.60	37.62	1.19	3.65	vOH(99)
2	A'			3704	3720	3376	3368	81.60	61.29	5.50	13.60	vOH(98)
3	A'		3066	3222	3214	3068	3068	3.92	3.90	4.57	11.32	vCH(98)
4	A'		3006	3204	3192	3008	3005	16.71	22.91	13.10	36.25	vCH(97)
5	A'	2992		3190	3179	2990	2995	23.50	29.77	5.44	14.69	vCH(96)
6	A'		2982	3186	3176	2982	2980	2.31	2.30	3.39	9.21	vCH(95)
7	A'		2912	3175	3165	2915	2913	0.36	0.43	2.29	5.75	vCH(95)
8	A'			3142	3130	2902	2900	16.72	17.88	2.62	6.83	vCH(94)
9	A'		1681	1784	1756	1682	1680	393.62	523.06	18.70	90.53	vC=O(83), δOH(10)
10	A'	1633	1634	1679	1669	1630	1632	53.88	59.48	11.75	43.17	vCC(92)
11	A'		1607	1654	1648	1614	1610	21.36	21.09	3.55	11.31	vCC(91)
12	A'	1572	1577	1625	1615	1578	1575	19.43	14.25	4.34	16.62	vCC(78), δOH (12)
13	A'	1505	1506	1553	1551	1508	1506	47.44	34.69	0.15	1.24	vCC(88), δCH (7)
14	A'		1466	1499	1506	1470	1467	29.18	25.33	30.53	78.64	vCC(69), δCH (17), δOH (6)
15	A'	1452		1467	1465	1454	1450	142.29	65.41	23.80	56.58	vCC(75), δOH (17)
16	A'	1430		1451	1442	1436	1432	15.72	41.52	7.10	13.64	vC-O(78), δCH (14)
17	A'	1412	1414	1425	141	1410	1413	79.16	196.90	86.10	78.18	vC-O(76), δCH(11)
18	A'	1386	1382	1404	1387	1390	1366	85.21	56.08	19.30	96.35	vCC(79), vC-O(12)
19	A'	1352		1369	1366	1352	1350	77.72	63.32	0.39	2.32	vCC(75), δOH (16)
20	A'		1320	1294	1305	1328	1325	22.10	26.10	3.28	8.93	vCC(76), δCH (12)
21	A'	1305		1277	1281	1310	1308	57.05	30.30	0.91	2.78	vCC(78), δCH(12), δOH (6)
22	A'	1256	1257	1240	1238	1260	1258	11.53	33.66	0.88	1.98	vCC(74), δCH(12)
23	A'	1217	1216	1222	1226	1220	1217	137.61	125.05	5.57	10.16	vCC(78), δOH (12)
24	A'		1178	1206	1210	1180	1178	35.94	59.58	14.78	73.91	δOH (81), δCH (11)
25	A'	1090		1187	1200	1094	1092	23.88	27.77	1.52	7.67	δOH (84)
26	A'	1023		1164	1176	1028	1025	2.74	9.28	3.54	8.16	δCH(78)
27	A'		981	1138	1135	983	980	210.14	251.05	0.40	0.38	δCO(75), δCH(22)
28	A'	954		1102	1102	960	955	1.48	16.44	0.38	1.78	δCO(75)
29	A'	912	916	1057	1055	922	915	3.58	4.05	9.77	40.89	R1 <sub>irigd</sub> (67) δCH(25)
30	A'	877	876	1009	1000	882	877	0.00	0.07	0.11	0.50	δCH(78)
31	A'	870		1002	988	874	868	0.17	0.65	0.01	0.36	δCH(77)
32	A'	794		955	940	802	795	1.01	1.45	0.23	1.22	δCH(73), γCC(21)
33	A'	762		904	903	769	764	5.72	3.61	0.01	0.33	R2 <sub>irigd</sub> (65)
34	A'	722	722	881	884	726	720	8.13	12.98	1.34	6.47	R2 <sub>sym</sub> (69)
35	A'	708		879	866	714	710	12.33	15.92	1.38	1.07	R1 <sub>asym</sub> (68)
36	A'			851	850	708	700	0.68	0.08	0.83	1.30	δCC(68), δCH(19)
37	A'			809	801	686	681	17.29	38.87	0.84	0.62	δCH(79), δOH(16)
38	A'			785	778	670	663	72.87	88.35	0.47	1.04	δCH(65), δCO(19), δOH(7)
39	A'	655		746	742	662	659	2.78	41.36	3.28	21.50	δCO(69),
40	A'			740	736	640	632	34.81	9.33	8.20	0.46	R2 <sub>asym</sub> (63), γ OH(23)
41	A'	604	600	712	713	608	602	26.61	22.78	13.85	52.96	R1 <sub>sym</sub> (79)
42	A''	571		684	668	575	570	8.24	2.60	3.32	1.84	γ OH(68), γCH(27)
43	A''			620	622	568	562	7.00	7.12	0.60	1.56	R1 <sub>irigd</sub> (65), δCO(21)
44	A''			615	594	552	549	77.98	25.44	4.55	10.50	γCH (67), γCH(27)
45	A''		538	592	582	547	539	25.11	60.43	3.33	0.25	γ R1 <sub>asym</sub> (58), γCH(17)
46	A''	492		586	571	499	495	2.13	54.72	3.01	7.05	γ OH(54)
47	A''		488	536	538	490	485	22.04	23.14	8.88	30.75	γ R1 <sub>irigd</sub> (55), γCH(19)
48	A''	464		491	489	468	463	1.98	3.19	1.39	22.07	γ CH(51), γ OH(34)
49	A''		413	489	482	415	412	2.82	11.45	7.55	2.11	γ R2 <sub>irigd</sub> (51)
50	A''		350	437	429	358	352	15.24	10.66	1.22	2.50	γ CH(53)
51	A''		325	390	390	330	326	1.25	1.06	2.04	6.48	γ CO(57)
52	A''			340	343	316	312	0.82	1.30	12.17	31.06	γ R2 <sub>asym</sub> (54)
53	A''		288	327	327	292	290	1.54	1.39	9.45	32.12	γ R2 <sub>sym</sub> (52)
54	A''		263	293	281	267	265	6.78	4.15	2.43	0.93	γ CH(49)
55	A''		225	267	218	228	226	54.86	0.68	4.38	1.78	γ CH(48)
56	A''		188	221	205	193	189	1.03	2.01	5.00	5.08	Ring Butterfly(59), γOH(35)
57	A''		163	193	179	160	162	2.07	1.67	2.26	26.79	γ CC(49), γOH(33)
58	A''		71	91	67	72	70	6.76	0.04	18.00	10.00	γ CH(48)
59	A''			58	42	43	40	4.86	0.31	87.03	10.12	γ CO(47), γCH(21)
60	A''			48	40	41	38	0.00	62.32	4.16	46.16	γ CO(44)

A': In-plane; A'': out-of-plane; sym: symmetric stretching; asym: asymmetric stretching; v: stretching; δ: in-plane bending; γ: out-of-plane bending; t: torsion; wagg: wagging; sciss: scissoring; τ: twisting; sb: symmetric bending; ipb: in-plane-bending; opb: out-plane-bending; ipr: in-plane-rocking; opr: out-plane-rocking;

**Table 3. The charge distribution calculated by the Mulliken and natural bond orbital (NBO) methods using DFT/B3LYP/ccPVDZ of 1-hydroxy naphthalene 2-carboxylic acid molecule.**

Atoms	DFT	
	Atomic charges(Mulliken)	Natural charges(NBO)
C1	0.037255	0.41981
C2	-0.087279	-0.23551
C3	0.085837	-0.16698
C4	0.032504	-0.23093
C5	0.041922	-0.18803
C6	0.060916	-0.20842
C7	0.064574	-0.21319
C8	0.007393	-0.20767
C9	0.045051	-0.11788
C10	0.011458	-0.03745
O11	-0.068177	-0.63517
H12	0.125408	0.47337
C13	0.188697	0.85065
O14	-0.256806	-0.62411
O15	-0.147283	-0.70205
H16	0.140396	0.48059
H17	0.038109	0.24301
H18	-0.055490	0.22509
H19	-0.048765	0.22592
H20	-0.035217	0.22603
H21	-0.038841	0.22570
H22	-0.065443	0.19722

The NBO method demonstrates the bonding concepts like atomic charge, Lewis structure, bond type, hybridization, bond order, and charge transfer and resonance possibility. Natural bond orbital (NBO) analysis is a useful tool for understanding delocalization of electron density from occupied Lewis-type (donor) NBOs to properly unoccupied non-Lewis type (acceptor) NBOs within the molecule. The stabilization of orbital interaction is proportional to the energy difference between interacting orbitals. Therefore, the interaction having strongest stabilization takes place between effective donors and effective acceptors. This bonding, anti-bonding interaction can be quantitatively described in terms of the NBO approach that is expressed by means of second-order perturbation interaction energy  $E^{(2)}$  [35]. This energy represents the estimate of the off-diagonal NBO Fock matrix element. The stabilization energy  $E^{(2)}$  associated with  $i$  (donor)  $\rightarrow$   $j$  (acceptor) delocalization is estimated from the second-order perturbation approach as given below

$$E^{(2)} = q_i \frac{F^2(i, j)}{\epsilon_j - \epsilon_i}$$

Where  $q_i$  is the donor orbital occupancy,  $\epsilon_i$  and  $\epsilon_j$  are diagonal elements (orbital energies) and  $F(i, j)$  is the off-diagonal Fock matrix element. The second order perturbation analyses of Fock matrix of 1HN2CA are summarized in Table 4. The Fock matrix analysis yields different types of donor-acceptor interactions and their stabilization energy. All lone pair-bond pair interactions and only bond pair-bond pair interactions with stabilization energies are listed in Table 4. In 1HN2CA molecule, the lone pair donor orbital, LPO15  $\rightarrow$   $\pi^*$ C13-O14 interaction between the O15 lone pair and the C13-O14 antibonding orbital is seen to give a strong stabilization, 45.86 kJ mol<sup>-1</sup> and LP14  $\rightarrow$   $\pi^*$ C13-O15 interaction has the stabilization energy of 30.62 kJ mol<sup>-1</sup>. These stabilization energies of lone pair-bond pair and bond pair-bond pair interactions are give more stabilization than other interactions. The  $\pi$  electron cloud movement from donor

to acceptor can make the molecule highly polarized and the 1HN2CA is present and it must be responsible for the NLO properties.

The NBO analysis also describes the bonding in terms of the natural hybrid orbital LPO15, which occupy a higher energy orbital with considerable p-character (57.31%) and low occupation number (1.97479 a.u.) and the other LPO14 occupy a lower energy orbital with p-character (41.07%) and high occupation number (1.97419 a.u.). Thus, a close to pure p-type lone pair participates in the electron donation to the  $\sigma^*$  C2-C1, and  $\sigma^*$  C2-C3 orbital for LPO14  $\rightarrow$   $\sigma^*$  C-C interaction in the compound. The other natural hybrid orbital interactions are presented in Table 4.

#### Frontier Molecular Orbitals and Atomic Charges

The most important orbital's in molecule is the frontier molecular orbital's, called highest occupied molecular orbital (HOMO) and lowest unoccupied molecular orbital (LUMO). These orbitals determine the way the molecule interacts with other species. The frontier orbital gap helps to characterize the chemical reactivity and kinetic stability of the molecule. A molecule with a small frontier orbital gap is more polarizable and is generally associated with a high chemical reactivity, low kinetic stability and is also termed as soft molecule [36]. The low values of frontier orbital gap in 1HN2CA make it more reactive and less stable. The HOMO is the orbital that primarily acts as an electron donor and the LUMO is the orbital that largely acts as the electron acceptor. The 3D plot of the frontier orbital's HOMO and LUMO for 1HN2CA molecule are shown in Fig. 4. The positive phase is red and the negative one is green (For interpretation of the references to color in this text, the reader is referred to the web version of the article). Many organic molecules, containing conjugated p electrons are characterized by large values of molecular first hyperpolarizabilities, were analyzed by means of vibrational spectroscopy [37, 38]. In most cases, even in the absence of inversion symmetry, the strongest band in the FT-Raman spectrum is weak in the FT-IR spectrum vice versa. But the intra-molecular charge transfer from the donor to acceptor group through a single-double bond conjugated path can induce large variations of both the molecular dipole moment and the molecular polarizability, making FTIR and FT-Raman activity strong at the same time. The experimental spectroscopic behavior described above is well accounted by ab initio calculations in p conjugated systems that predict exceptionally large Raman and IR intensities for the same normal modes [38]. It is also observed in our title molecule the bands in FTIR spectrum have their counterparts in FT-Raman shows that the relative intensities in FTIR and FT-Raman spectra are comparable resulting from the electron cloud movement through  $\pi$  conjugated frame work from the electron donor to electron acceptor groups. The analysis of the wave function indicates that the electron absorption corresponds to the transition from the ground to the first excited state and is mainly described by one-electron excitation from the highest occupied molecular orbital (HOMO) to the lowest unoccupied molecular orbital (LUMO). The HOMO of  $\pi$  nature, (i.e., benzene ring) is delocalized over the C-C bond. By contrast, LUMO is located over hydroxyl, and oxygen atoms of carboxylic acid group. It can be seen from the Fig. 4 that, the HOMO is distributed in ring and hydroxyl group of title molecule.

The LUMO in C2-C13 and O14 of carboxylic acid group are found to spread over the ring. All the HOMO and LUMO

have nodes. The nodes in each HOMO and LUMO are placed symmetrically.

The energy gap of HOMO–LUMO explains the eventual charge transfer interaction within the molecule, which influences the NLO activity of the molecule. As the energy gap between the LUMO and HOMO decreases, it is easier for the electrons of the HOMO to be excited. The higher the energy of HOMO, the easier it is for HOMO to donate electrons whereas it is easier for LUMO to accept electrons when the energy of LUMO is low. The energy values of HOMO and LUMO levels are computed to be -0.21767 a.u. and -0.05650 a.u., respectively, and the energy difference is 0.16117 a.u.

The calculation of atomic charges plays a key role in the application of quantum mechanical calculation to describe the electronic characteristics of molecular systems [39]. A comparative study of the NBO and Mullikan atomic charge distributions in 1-hydroxynaphthalene-2-carboxylic acid, determined on the basis of quantum mechanical method with B3LYP method is presented in Table 3.

Both Mullikan's atomic net charges [40–42] and the natural NBO/NPA atomic charges were calculated. The results are listed in Table 3. Regarding the molecular symmetries only the charges of 22 atoms are listed for title molecule. The comparison between Mullikan's net charges and the atomic natural one is not an easy task since the theoretical background of the two methods was very different. Looking at the results there are surprising differences between the Mullikan's and the NBO charges. All of the NBO charges have the negative sign for C2 atom and positive sign for C1 atom on the B3LYP method, whilst the Mullikan's values for the C1 and C2 atoms are same in sign as compared to these values for the method. The definition of Mullikan's charges is based on population analysis. The Mullikan population analysis provides a partitioning of either the total charge density or an orbital density. The number of electrons in molecule (N) is the integral of the charge density over the space. N is partitioned for all atoms considering also the overlap population. According to the theory the overlap population of atoms A and B is divided between the two atoms in half-to-half ratio. This is one weak point of the theory. The other weak point is its strong dependence on the basis set applied. The Mullikan's atomic net charges are presented in Table 3.

Molecular electrostatic used extensively for interpreting potentials have been and predicting the reactive behavior of a wide variety of chemical system in both electrophilic and nucleophilic reactions, the study of biological recognition processes and hydrogen bonding interactions [43].  $V(r)$ , at a given point  $r(x, y, z)$  in the vicinity of a compound, is defined in terms of the interaction energy between the electrical charge generated from the compound electrons and nuclei and positive test charge (a proton) located at  $r$ . Unlike, many of the other quantities used at present, and earlier as indices of reactivity  $V(r)$  is a real physical property that can be determined experimentally by diffraction or by computational methods. For the systems studied the MEP values were calculated as described previously, using the equation [44]

$$V(r) = \sum \frac{Z_A}{|R_A - r|} - \int \frac{\rho(r')}{|r' - r|} dr$$

Where the summation runs over all the nuclei A in the compound and polarization and reorganization effects is

neglected.  $Z_A$  is the charge of the nucleus A, located at R and  $q(r')$  is the electron density function of the compound.

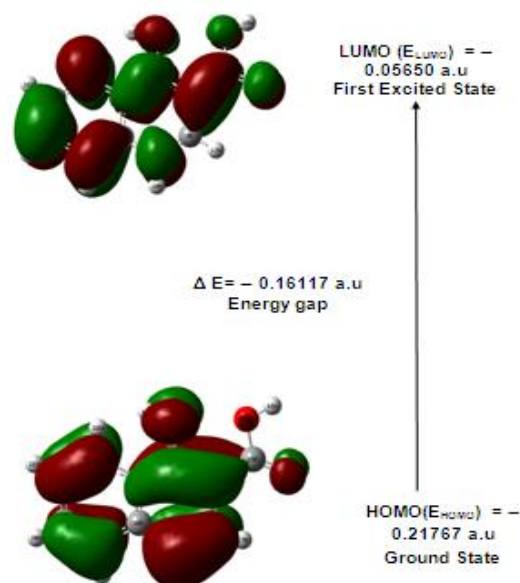


**Fig 4. The atomic orbital composition of the molecular orbital for 1- F hydroxy naphthalene 2-carboxylic acid. Molecular electrostatic potentials (MEPs)**

To predict reactive sites for electrophilic and nucleophilic attack for the investigated compound, molecular electrostatic potential (MEP) was calculated at B3LYP/ccPVDZ optimized geometries. Red and blue areas in the MEP map refer to the electron-rich and electron-poor regions, respectively, whereas the green color signifies the neutral electrostatic potential. The MEP surface provides necessary information about the reactive sites. The electron total density onto which the electrostatic potential surface has been mapped is shown in Fig. 5.

The negative regions  $V(r)$  were related to electrophilic reactivity and the positive ones to nucleophilic reactivity. As easily can be seen in Fig. 5, this compound has several possible sites for electrophilic attack in which  $V(r)$  calculations have provided in-sights.. Thus, it would be predicted that an electrophile would preferentially attack 1HN2CA at the oxygen atoms of carboxyl, and hydroxyl position.

Alternatively, we found the positive regions over the hydrogen atoms of 1HN2CA compound and indicating that these sites can be the most probably involved in nucleophilic processes.

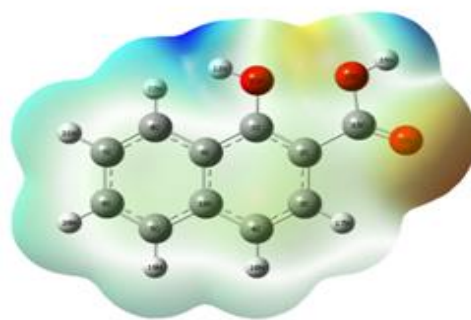


**Fig 5. DFT (B3LYP)/ccPVDZ calculated 3D molecular electrostatic potential of 1-hydroxy naphthalene 2-carboxylic acid.**

Table 4. Second-order perturbation theory analysis of Fock matrix in NBO basic corresponding to the intra molecular bonds of 1-hydroxy naphthalene 2-carboxylic acid.

Donor (i)	ED (i) (e)	Acceptor (j)	ED (j) (e)	<sup>a</sup> E <sup>(2)</sup> (kJ mol <sup>-1</sup> )	<sup>b</sup> E(j) – E(i) (a.u.)	<sup>c</sup> F(i,j) (a.u.)
σ(C <sub>1</sub> –C <sub>2</sub> )	1.96540	σ*(C <sub>1</sub> –C <sub>9</sub> )	0.03846	4.65	1.29	0.069
π(C <sub>6</sub> –C <sub>7</sub> )	1.68556	π*(C <sub>3</sub> –C <sub>4</sub> )	0.24174	19.82	0.32	0.072
σ(C <sub>1</sub> –C <sub>9</sub> )	1.96924	σ*(C <sub>1</sub> –C <sub>2</sub> )	0.03210	5.34	1.33	0.075
σ(C <sub>1</sub> –O <sub>11</sub> )	1.99256	σ*(C <sub>2</sub> –C <sub>3</sub> )	0.01995	2.22	1.57	0.053
σ(C <sub>2</sub> –C <sub>3</sub> )	1.96920	σ*(C <sub>1</sub> –C <sub>2</sub> )	0.03210	4.65	1.31	0.070
σ(C <sub>2</sub> –C <sub>13</sub> )	1.96984	σ*(C <sub>1</sub> –C <sub>9</sub> )	0.03846	3.93	1.20	0.061
σ(C <sub>3</sub> –C <sub>4</sub> )	1.97961	σ*(C <sub>5</sub> –C <sub>10</sub> )	0.02397	3.56	1.26	0.060
π(C <sub>3</sub> –C <sub>4</sub> )	1.75715	π*(C <sub>9</sub> –C <sub>10</sub> )	0.46844	19.02	0.29	0.070
σ(C <sub>4</sub> –C <sub>10</sub> )	1.97223	σ*(C <sub>5</sub> –C <sub>10</sub> )	0.02397	3.31	1.23	0.057
σ(C <sub>4</sub> –H <sub>18</sub> )	1.97955	σ*(C <sub>9</sub> –C <sub>10</sub> )	0.03420	4.70	1.09	0.064
π(C <sub>5</sub> –C <sub>6</sub> )	1.73303	π*(C <sub>7</sub> –C <sub>8</sub> )	0.26405	18.40	0.29	0.066
σ(C <sub>5</sub> –C <sub>10</sub> )	1.97244	σ*(C <sub>9</sub> –C <sub>10</sub> )	0.03420	3.67	1.26	0.061
σ(C <sub>5</sub> –H <sub>19</sub> )	1.97986	σ*(C <sub>9</sub> –C <sub>10</sub> )	0.03420	4.66	1.10	0.064
σ(C <sub>6</sub> –C <sub>7</sub> )	1.97676	σ*(C <sub>8</sub> –H <sub>22</sub> )	0.01654	3.28	1.15	0.055
σ(C <sub>6</sub> –H <sub>20</sub> )	1.98037	σ*(C <sub>5</sub> –C <sub>10</sub> )	0.02397	4.67	1.08	0.064
σ(C <sub>7</sub> –C <sub>8</sub> )	1.97774	σ*(C <sub>8</sub> –C <sub>9</sub> )	0.02519	3.78	1.27	0.062
π(C <sub>7</sub> –C <sub>8</sub> )	1.75370	π*(C <sub>5</sub> –C <sub>6</sub> )	0.24251	17.00	0.31	0.065
σ(C <sub>7</sub> –H <sub>21</sub> )	1.98059	σ*(C <sub>8</sub> –C <sub>9</sub> )	0.02519	4.84	1.08	0.065
σ(C <sub>8</sub> –C <sub>9</sub> )	1.97086	σ*(C <sub>9</sub> –C <sub>10</sub> )	0.03420	4.23	1.26	0.065
π(C <sub>9</sub> –H <sub>10</sub> )	1.56575	π*(C <sub>1</sub> –C <sub>2</sub> )	0.36368	25.52	0.29	0.073
σ(O <sub>11</sub> –H <sub>12</sub> )	1.98321	σ*(C <sub>1</sub> –C <sub>2</sub> )	0.03210	6.56	1.38	0.085
π(C <sub>13</sub> –O <sub>14</sub> )	1.98740	π*(C <sub>1</sub> –C <sub>2</sub> )	0.36368	3.28	0.40	0.036
σ(C <sub>13</sub> –O <sub>15</sub> )	1.98621	σ*(C <sub>2</sub> –C <sub>3</sub> )	0.07154	4.41	1.12	0.047
σ(O <sub>15</sub> –H <sub>16</sub> )	1.99621	σ*(C <sub>2</sub> –C <sub>13</sub> )	0.01995	1.84	1.49	0.064
LP(1)O11	1.97214	σ*(C <sub>1</sub> –C <sub>9</sub> )	0.03846	7.32	1.14	0.082
LP(1)O14	1.97419	σ*(C <sub>2</sub> –C <sub>13</sub> )	0.07154	3.03	1.07	0.051
LP(1)O15	1.97479	σ*(C <sub>13</sub> –O <sub>14</sub> )	0.26242	5.22	1.15	0.069
LP(2)O11	1.82180	π*(C <sub>1</sub> –C <sub>2</sub> )	0.36368	41.08	0.37	0.115
LP(2)O14	1.84488	π*(C <sub>13</sub> –C <sub>15</sub> )	0.09469	30.62	0.60	0.123
LP(2)O15	1.81288	π*(C <sub>13</sub> –O <sub>14</sub> )	0.26242	45.86	0.33	0.112

<sup>a</sup>E(2) means energy of hyper conjugative interactions.

<sup>b</sup>E Energy difference between donor and acceptor i and j NBO orbital's.

<sup>c</sup>F(i,j) is the Fock matrix element between i and j NBO orbital's.

### Thermodynamic Properties

On the basis of vibrational analysis, the statically thermodynamic functions: heat capacity (C<sub>p</sub>), enthalpy changes (ΔH), Gibb's free energy (Δ) and entropy (S<sup>0</sup><sub>m</sub>) for the title molecule were obtained from the theoretical harmonic frequencies and listed in Table 5. From the Table 5, it can be observed that these thermodynamic functions are increasing with temperature ranging from 100 to 1000 K due to the fact that the molecular vibrational intensities increase with temperature. The correlation equations between heat capacity, Gibb's free energy, entropy, enthalpy changes and temperatures were fitted by quadratic formulas and the corresponding fitting factors (R<sup>2</sup>) for these thermodynamic properties are 0.9995, 0.9996, 1.0000 and 0.998, respectively. The corresponding fitting equations are as follows and the correlation graphics of those shown in Figs. 6.

All the thermodynamic data supply helpful information for the further study on the 1HN2CA. They can be used to compute the other thermodynamic energies according to relationships of thermodynamic functions and estimate directions of chemical reactions according to the second law of thermodynamics in thermo chemical field. Notice: all thermodynamic calculations were done in gas phase and they could not be used in solution.

In addition to the vibrational assignments, several thermodynamic parameters, rotational constants, and dipole moment have been presented in Table 6. The self consistent field (SCF) energy, zero point vibrational energies (ZPVEs),

rotational constants and entropy S<sub>vib</sub>(T) are calculated to the extent of accuracy and variations in the ZPVEs seem to be insignificant [45]. Dipole moment reflects the molecular charge distribution and is given as a vector in three dimensions. Therefore, it can be used as descriptor to depict the charge movement across the molecule. Direction of the dipole moment vector in a molecule depends on the centers of positive and negative charges. Dipole moments are strictly determined for neutral molecules. For charged systems, its value depends on the choice of origin and molecular orientation.

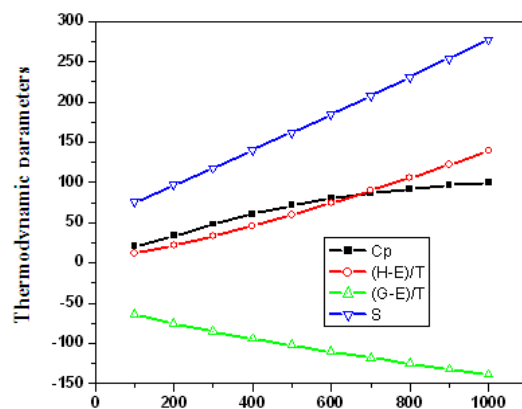


Fig 6. Correlation graphic of thermodynamic parameters and temperature for 1-hydroxy naphthalene 2-carboxylic acid.

**Table 5. Thermodynamic functions of 1-hydroxy naphthalene 2-carboxylic acid.**

Temp(K)	Cp (Cal Mol <sup>-1</sup> K <sup>-1</sup> )	(H-E)/T (Cal Mol <sup>-1</sup> K <sup>-1</sup> )	(G-E)/T (Cal Mol <sup>-1</sup> K <sup>-1</sup> )	S (Cal Mol <sup>-1</sup> K <sup>-1</sup> )
100	20.31	12.26	-63.86	76.11
200	33.84	21.70	-75.55	97.25
300	48.05	33.14	-85.14	118.28
400	60.86	45.94	-93.95	139.89
500	71.39	59.79	-102.27	162.06
600	79.74	74.49	-110.19	184.68
700	86.38	89.88	-117.76	207.63
800	91.73	105.84	-124.97	230.81
900	96.13	122.28	-131.86	254.14
1000	99.80	139.12	-138.43	277.55

**Table 6. Thermodynamic functions of 1-hydroxy naphthalene 2-carboxylic acid.**

Parameter	B3LYP/ccPVDZ
Self consistent field energy	-649.7278 a.u
Zero point vibrational energy	104.29928(kcal/mol)
Rotational constants	1.67263 GHz
	0.46886 GHz
	0.36621 GHz
Entropy	104.348 cal/mol K
Specific heat capacity at constant volume	43.594 cal/mol K
Translational energy	41.601cal/mol K
Rotational energy	31.393 cal/mol K
Vibrational energy	31.354 cal/mol K

$$(C_p^0) = 3.213 + 17.37T - 0.7781T^2 (R^2 = 0.9995)$$

$$(S^0) = 55.361 + 20.5T - 0.1747T^2 (R^2 = 1)$$

$$(H - E/T) = 1.3067 + 9.5827T + 0.4268T^2 (R^2 = 0.998)$$

$$(G - E/T) = -56.061 - 10.91T + 0.252T^2 (R^2 0.9996)$$

All the thermodynamic data supply helpful information for the further study on the 1HN2CA. They can be used to compute the other thermodynamic energies according to relationships of thermodynamic functions and estimate directions of chemical reactions according to the second law of thermodynamics in thermo chemical field. Notice: all thermodynamic calculations were done in gas phase and they could not be used in solution.

In addition to the vibrational assignments, several thermodynamic parameters, rotational constants, and dipole moment have been presented in Table 6. The self consistent field (SCF) energy, zero point vibrational energies (ZPVEs), rotational constants and entropy  $S_{\text{vib}}(T)$  are calculated to the extent of accuracy and variations in the ZPVEs seem to be insignificant [45]. Dipole moment reflects the molecular charge distribution and is given as a vector in three dimensions. Therefore, it can be used as descriptor to depict the charge movement across the molecule. Direction of the dipole moment vector in a molecule depends on the centers of positive and negative charges. Dipole moments are strictly determined for neutral molecules. For charged systems, its value depends on the choice of origin and molecular orientation.

### Conclusion

In this study, some experimental investigations and theoretical results were used to clarify the identification of 1-hydroxy naphthalene 2-carboxylic acid. The optimized molecular structure (bond lengths and bond angles), vibrational frequencies including Infrared intensities and

Raman intensities were derived from the computed Raman scattering activities, corresponding vibrational spectra interpreted with the aid of normal coordinate analysis based on scaled an density functional force field, thermodynamic properties and atomic charges were analyzed utilizing B3LYP/ccPVDZ method. It was found that the optimized molecular structures and vibrational frequencies were shown to have a good agreement with available experimental results and the chosen calculation level is powerful approach for understanding the molecular structure and vibrational spectra of the 1-hydroxy naphthalene 2-carboxylic acid. The MEP map shows that the negative potential sites are on electronegative atoms as well as the positive potential sites are around the hydrogen atoms. These sites give information about the region from where the compound can have intramolecular interactions. In addition, not only were HOMO and LUMO orbital's visualized and interpreted but also transition state and energy band gap were investigated for identification of the title compound. The NBO analysis is more compatible with the molecular structure of the title compound and it is a very useful method for molecular modeling. In conclusion this study not only shows the way to the characterization of the molecule but also helps to researchers for the future studies in technology and industry.

### References

- [1] Parr R G, Yang W, Density Functional Theory of Atoms and Molecules, Oxford, New York, 1989.
- [2] Jones R O, Gunnarson O, Rev. Mol. Phys. 1989 61 689.
- [3] Ziegler T, Chem. Rev. 1991 91 651.
- [4] Kohn W, Sham L. J, Phys. Rev. A 1965 140 1133.
- [5] Pulay P, Fogarasi G, Zhou X, Taylor P,W. Vib. Spectroscopy. 1990 1 159.
- [6] Kramers H A, Heisenberg W, Z. Phys. 1925 31 681.
- [7] Martin J M L, Alsenoy C V, J. Phys. Chem. 1996 100 6973.
- [8] Martin J M L, Yazal J E, Francis J P, J. Phys. Chem. 1996 100 15358.
- [9] Zhengyu Z, Dongmei Du, J. Mol. Struct. (Theochem) 2000 505 247.
- [10]Z. Zhengyu, Fu. Aiping, Du. Dongmei, Int. J. Quant. Chem. 2000 78 186.
- [11]Frisch M J, Trucks G W, Schlegel H B, Scuseria G E, Robb M A et al., Gaussian 09, Revision A. 02, Gaussian Inc., Wallingford, CT, 2009.
- [12]Frisch A, Niesen A B, Holder A J, Gauss View Users Manual, Gaussian Inc.,2008.
- [13]Reed A E, Weinhold F, J. Chem. Phys. 1985 83 1736–1740.
- [14]Snehalatha M, Ravi Kumar C, Hubert Joe I, Jaya Kumar V S, J. Raman Spectrosc. 2009 40 1121–1126.

- [15] Hubert Joe I, Kostova I, Ravi Kumar C, Amalanathan M, Pinzaru S C, J. Raman Spectrosc. 2009 40 1033–1038.
- [16] Ledesma A E, Zinczuk J, Ben Altabef A, Lopez Gonzalez J J, Brandan S A, J Raman Spectrosc. 2009 40 1004–1010.
- [17] Silverstein M, Clayton Basseler G, Morill C, Spectrometric Identification of Organic Compound, Wiley, New York, 1981 2560.
- [18] Krishnakumar V, Balachandran V, Chithambarathanu T, Spectrochim. Acta, Part A 2005 62 918–925.
- [19] Puviarasan N, Arjunan V, Mohan S, Turk J. Chem. 2002 26 323–334.
- [20] Varsanyi, Vibrational Spectra of Benzene Derivatives, Academic Press, New York, 1969.
- [21] Krishnakumar V, John Xavier R, Indian J. Pure Appl. Phys. 41 2003 597–602.
- [22] Krishnakumar V, Prabavathi V N, Spectrochim. Acta, Part A 71 2008 449–457.
- [23] Altun A, Golcuk K, Kumru M, J. Mol. Struct. 637 2003 155–169.
- [24] Sathiyarayanan D N, Vibrational Spectroscopy Theory and application, New age International Publishers: New Delhi. 2004
- [25] Gunasekaran S, Sailatha Indian E Journal of Pure and Applied Physics 47, 2009 259.
- [26] Fu A, Du D, Zhou Z, spectrochemica Acta Part A 59 2003 245.
- [27] Michalska D, Bienko D C, Abkowicz-Bienko A J, Latajka Z, J. Phys. Chem. 100 1996 17786–17790.
- [28] Varsanyi G, Assignments of Vibrational Spectra of Seven Hundred Benzene Derivatives, vols. 1–2, Adam Hilger, 1974.
- [29] Nuquist R.A, Spectrochim. Acta 19 1963 1655–1664.
- [30] Vein D.L, Colthup N B, Fateley W G, Grasselli J G, The Handbook of Infrared and Raman Characteristic Frequencies of Organic Molecules, Academic Press, San Diego, 1991.
- [31] Smith B, Infrared Spectral Interpretation, A Systematic Approach, CRC Press, Washington, DC, 1999.
- [32] Silverstein R M, Webster F X, Spectrometric Identification of Organic Compounds, sixth ed., John Wiley & Sons Inc., New York, 2003.
- [33] Keresztury G, Holly S, Varga J, Besenyi G, Wang A Y, Durig J R, Spectrochim. Acta 49A 1993 2007–2026.
- [34] Ahmad S, Mathew S, Verma P K, Indian J. Pure Appl. Phys. 30 1992 764–765.
- [35] Foster J P, Weinhold F, Am J. Chem. Soc. 102 1980 7211–7218.
- [36] Powell B J, Baruah T, Bernstein N, Brake K, McKenzie R H, Meredith P, Pederson M R, J. Chem. Phys. 120 2004 8608–8615.
- [37] Ataly Y, Avci D, Basoglu A, J. Struct. Chem. 19 2008 239–246.
- [38] Vijayakumar T, Hubert Joe I, Nair C P R, Jayakumar V S, J. Chem. Phys. 343 2008 83–99.
- [39] Xavier Assfeld, Rivail J L, Chem. Phys. Lett. 263 1996 100–106.
- [40] Mullikan R S, J. Chem. Phys. 23 1955 1833–1841.
- [41] Reed A E, Weinhold F J, Curtiss L A, Chem. Rev. 88 1988 899–926.
- [42] Parr R G, Szentpaly L V, Liu S J, Am. Chem. Soc. 121 1999 1922–1924.
- [43] Politzer P, Murray J S, Theoretical biochemistry and molecular biophysics: a comprehensive survey, in: Beveridge D L, Lavery R (Eds.), Electrostatic Potential Analysis of Dibenzo-p-dioxins and Structurally Similar Systems in Relation to their Biological Activities, Protein, vol. 2, Academic Press, Schenectady, NY, 1991 (Chapter 13).
- [44] Politzer P, Murray J, Theor. Chem. Acc. 108 2002 134–142.
- [45] Nagabalasubramanian P B, Periyandi S, Mohan S, Spectrochim. Acta, Part A 77 2010 150–159.